

Acoustic Signatures of the Helium Core Flash

Lars Bildsten, Bill Paxton, Kevin Moore, & Phillip J. Macias

*Kavli Institute for Theoretical Physics and Department of Physics
Kohn Hall, University of California, Santa Barbara, CA 93106*

ABSTRACT

All evolved stars with masses $M \lesssim 2M_{\odot}$ undergo an initiating off-center helium core flash in their $M_c \approx 0.48M_{\odot}$ He core as they ascend the red giant branch (RGB). This off-center flash is the first of a few successive helium shell subflashes that remove the core electron degeneracy over 2 Myrs, converting the object into a He burning star. Though characterized by Thomas over 40 years ago, this core flash phase has yet to be observationally probed. Using the Modules for Experiments in Stellar Astrophysics (MESA) code, we show that red giant asteroseismology enabled by space-based photometry (i.e. *Kepler* and CoRoT) can probe these stars during the flash. The rapid ($\lesssim 10^5$ yr) contraction of the red giant envelope after the initiating flash dramatically improves the coupling of the p-modes to the core g-modes, making the detection of $\ell = 1$ mixed modes possible for these 2 Myrs. This duration implies that 1 in 35 stars near the red clump in the HR diagram will be in their core flash phase. During this time, the star has a g-mode period spacing of $\Delta P_g \approx 70 - 100$ s, lower than the $\Delta P_g \approx 250$ s of He burning stars in the red clump, but higher than the RGB stars at the same luminosity. This places them in an underpopulated part of the large frequency spacing ($\Delta\nu$) vs. ΔP_g diagram that should ease their identification amongst the thousands of observed red giants.

Subject headings: stars: interiors — stars: oscillations — stars: late-type

1. Introduction

Sensitive space-based photometry from CoRoT (Baglin et al. 2009) and *Kepler* (Borucki et al. 2009) has enabled detection and characterization of radial and non-radial acoustic (i.e. p-mode) oscillations in thousands of red giant stars (De Ridder et al. 2009; Bedding et al. 2010; Huber et al. 2010; Mosser et al. 2010; Hekker et al. 2011; Miglio 2011) with frequencies centered at

$$\nu_{\max} \approx 31 \mu\text{Hz} \left(\frac{M}{M_{\odot}} \right) \left(\frac{10R_{\odot}}{R} \right)^2 \left(\frac{5777 \text{ K}}{T_{\text{eff}}} \right)^{1/2}, \quad (1)$$

consistent with the scaling of the acoustic cutoff frequency (Brown et al. 1991). These modes generate photometric variability ranging from 5 to 1000 parts per million (Mosser et al. 2011b; Huber et al. 2011) and have lifetimes of at least 15 days (Huber et al. 2010; Baudin et al. 2011). Their excitation and damping (and thereby their resulting amplitudes; Kjeldsen & Bedding (1995)) is related to the presence of vigorous convection within the star (see review by Christensen-Dalsgaard (2011a)). The majority of these oscillations are p-modes with nearly evenly spaced frequencies at

$$\Delta\nu \approx 4.27\mu\text{Hz} \left(\frac{M}{M_\odot}\right)^{1/2} \left(\frac{10R_\odot}{R}\right)^{3/2}, \quad (2)$$

a relation used with equation (1) to determine the stellar mass, M , and radius R from the measured ν_{max} , effective temperature T_{eff} and $\Delta\nu$ (Hekker et al. 2011). The implied relation between ν_{max} and $\Delta\nu$ has also been confirmed observationally (Stello et al. 2009; Hekker et al. 2009; Bedding et al. 2010; Huber et al. 2010; Hekker et al. 2011; Mosser et al. 2011b; Huber et al. 2011).

Space-based observations (Bedding et al. 2010; Beck et al. 2011; Mosser et al. 2011a) also enabled the detection of the angular degree $\ell = 1$ mixed modes, which have p-mode characteristics in the red giant envelope, but g-mode characteristics in the helium core (Scuflaire 1974; Osaki 1975; Aizenman et al. 1977; Dziembowski et al. 2001; Christensen-Dalsgaard 2004; Dupret et al. 2009; Montalbán et al. 2010). Modes nearly evenly spaced in period, at ΔP_{obs} , around the $\ell = 1$ p-modes were identified by Beck et al. (2011) as a characteristic of the interior core g-modes allowing Bedding et al. (2011) to distinguish first ascent red giant branch (RGB) stars (i.e. those with degenerate helium cores) from red clump stars (i.e. those with non-degenerate He burning cores). This separation in the $\Delta P_{\text{obs}} - \Delta\nu$ diagram was also seen by CoRoT (Mosser et al. 2011a), and is a powerful new tool for stellar population studies.

We show here that this new capability to probe the deep interior of a red giant should allow for the identification of those $M \lesssim 2M_\odot$ stars undergoing the helium core flash. Known for more than 40 years as the defining event that ends the ascent of low mass stars up the RGB (and defines the tip of the RGB; Salaris et al. (2002)), this thermally unstable and off-center helium burning leads to a $t_f \approx 2$ Myr phase of successive He subflashes (Thomas 1967; Iben & Renzini 1984; Mocák et al. 2008) that remove electron degeneracy and convert the He core to a stably burning non-degenerate object. However, there has been debate (see review by Iben & Renzini (1984)) as to whether the initiating flash can become dynamical in some way, or rather remains hydrostatic.

Using the MESA code (Paxton et al. 2011), we start in §2 by describing the changes in the red giant envelope and helium core during the core flash. We work in the Wentzel, Kramers,

Brillouin (WKB) approximation in §3, summarizing the p-mode and g-mode properties during the helium core flash. We close in §4 by discussing how stars in this phase of evolution can be differentiated from the more numerous populations of RGB and clump stars.

2. Stellar Evolution during the Core Flash Phase

Evolved stars with $M \lesssim 2.0M_{\odot}$ undergo a He core flash that ends their RGB evolution, and leads them to the red clump where they undergo core He burning for ≈ 70 Myrs. The flash starts as an off-center thermally unstable ignition of helium burning at a mass coordinate about half-way through the $M_c \approx 0.48M_{\odot}$ He core (Dominguez et al. 1999; Salaris et al. 2002; Serenelli & Weiss 2005; Serenelli & Fukugita 2005; Mocák et al. 2009; Paxton et al. 2011), nearly independent of metallicity and M .

Using MESA version 3709, we have calculated this evolution for a range of M , all with $X = 0.7$ and $Z = 0.02$, treating convection with the Schwarzschild criterion (i.e. no semi-convection, thermohaline mixing or convective overshoot) and a mixing length parameter of $\alpha_{\text{MLT}} = 2.0$. We had no mass loss, diffusion, or rotation and we used the MESA “basic” (Paxton et al. 2011) nuclear network with rates from NACRE. The opacity was from OPAL (Iglesias & Rogers 1996), with the low temperature opacities taken from Ferguson et al. (2005) with metal ratios given by Grevesse & Sauval (1998), as described in Paxton et al. (2011). We used the OPAL equation-of-state (Rogers & Nayfonov 2002), and HELM extensions (Timmes & Swesty 2000) where needed.

The evolutionary tracks in Figure 1 for a $M = 1.0M_{\odot}$ and $M = 1.8M_{\odot}$ star are for the time before, during, and after the core flash phase. The He core expansion from the initiating flash leads to an adiabatic temperature drop in the overlying H burning shell; quenching the burning. This loss of an energy source for the red giant envelope triggers a Kelvin-Helmholtz (KH) contraction from the tip of the RGB on a rapid timescale (Thomas 1967), reaching $L \approx 100 - 200L_{\odot}$ in 10^4 years (the open blue circles).

Thomas (1967) showed that the He core flash phase is governed by a series of shell subflashes that increase the entropy of the convective regions. This is seen in Figure 2, where five successive subflashes are seen to move inwards in mass coordinates. However, convective He burning is present for only about 10% of the time. The $t_f \approx 2$ Myr timescale is set by the need for thermal diffusion to act inwards between subflashes, ending when the thermal wave reaches the core (Thomas 1967; Serenelli & Weiss 2005), heating it at nearly constant pressure (Paxton et al. 2011) to the condition needed for the convective He burning core phase of the red clump. We end Figure 2 at that time. Even though the He burning

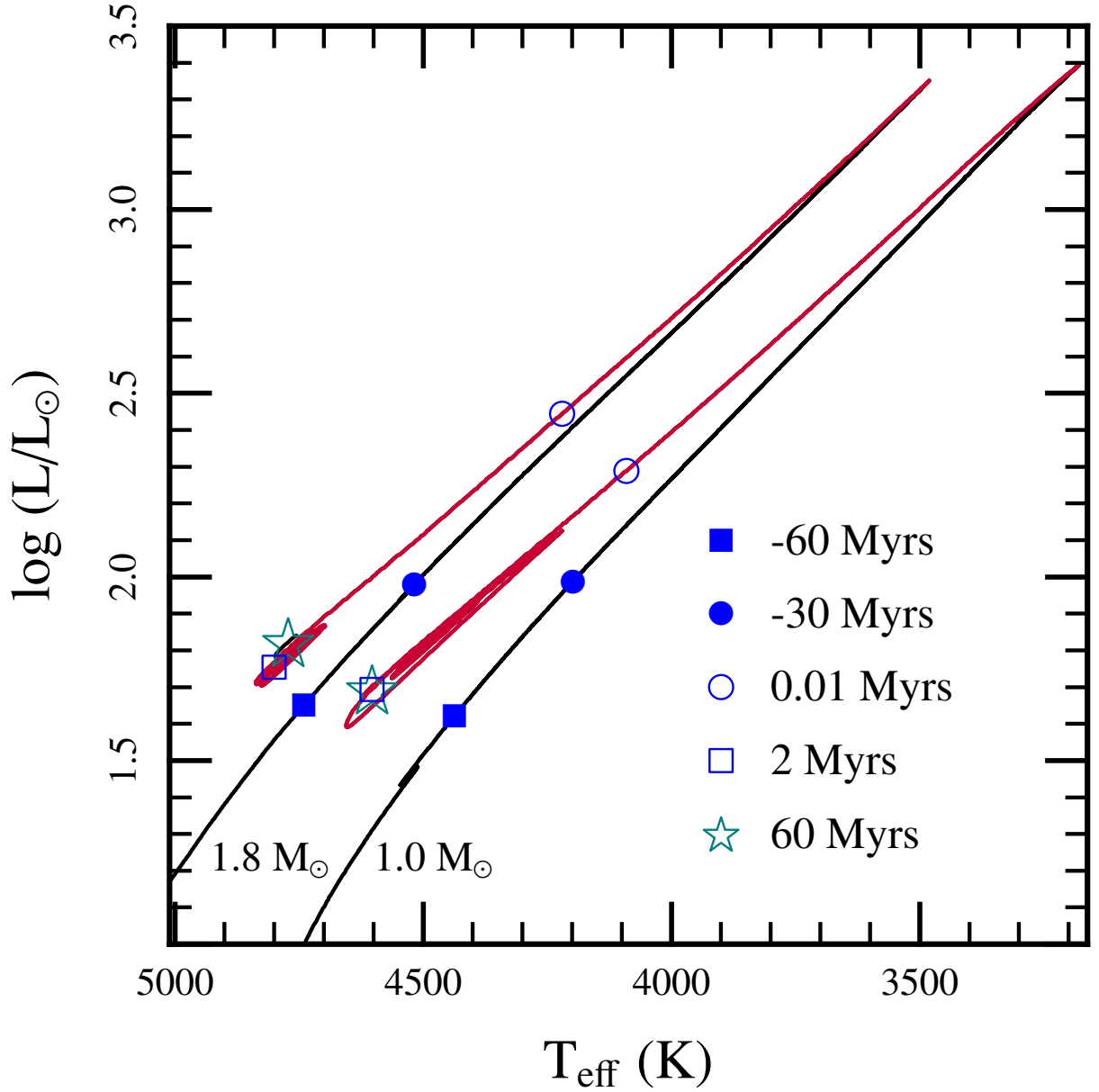


Fig. 1.— The evolution of a solar metallicity $M = 1.0M_{\odot}$ star and a $M = 1.8M_{\odot}$ star before (black line), during and after (red line) the core flash phase. The filled circles (squares) show where the star resided on the RGB at 30 (60) Myrs prior to the initiating flash at $L_{\text{tip}} = 10^{3.4}L_{\odot}$. The open circles show the location 0.01 Myr after the initiating flash, whereas the open blue square is 2 Myrs after the initiating flash, a time when the star reaches the red clump, where it still resides at 60 Myrs (green star).

luminosities (blue dashed lines) get quite large ($L_{\text{He}} \approx 10^{9.3} L_{\odot}$ in the initiating flash at $t = 0$), Shen & Bildsten (2009) have shown that the heating from He burning always occurs on a timescale much longer than the local dynamical time, an outcome confirmed in multi-dimensions by Mocák et al. (2008, 2009). The stellar response during the 2 Myr core flash phase is shown in Figure 2 and form the basis for our asteroseismological work.

3. Mode Properties during the Core Flash Phase

The non-radial adiabatic mode structures for RGB and red clump stars have been studied, with focus on the $\ell = 1$ mixed modes that reveal core properties (Dziembowski et al. 2001; Christensen-Dalsgaard 2004; Dupret et al. 2009; Montalbán et al. 2010; Christensen-Dalsgaard 2011a,b; Jiang et al. 2011; di Mauro et al. 2011). These mixed modes have a p-mode quality in the outer parts of the star (where they are excited by convection, and typically have $n_p \approx 10$ radial nodes), but penetrate into the stellar core as very high order ($n_g > 100$) g-modes. This justifies our initial exploration in the WKB limit (Unno et al. 1989; Aerts et al. 2010; Christensen-Dalsgaard 2011a), where the local (at radius r) radial wavenumber, k_r , is

$$k_r^2 = \frac{1}{c_s^2 \omega^2} (\omega^2 - N^2) (\omega^2 - S_\ell^2), \quad (3)$$

where $\omega = 2\pi\nu$ is the mode frequency, c_s is the sound speed, N^2 is the Brunt-Väisälä frequency, and $S_\ell^2 = c_s^2 \ell(\ell+1)/r^2$ is the Lamb frequency. Figure 3 shows the propagation diagrams (radial profiles of N , S_1 and S_2) for four phases of the $M = 1.0 M_{\odot}$ model, all chosen when $\Delta\nu = 4\mu\text{Hz}$. These resulted in nearly the same values of $\nu_{\text{max}} \approx 28\mu\text{Hz}$ (denoted by the horizontal line). From top to bottom, the panels are for $t = -60$ Myrs prior to the initiating flash (on the RGB), $t = 1.4$ Myrs (after the initiating flash), $t = 1.6$ Myrs (during a convective He burning subflash) and $t = 2.0$ Myrs when the star is in the convective He core burning phase of the red clump.

Modes supported by the acoustic response of the envelope (i.e. p-modes) propagate in the outer parts of the star where $\omega^2 > S_\ell^2$ and $\omega^2 > N^2$. Since N^2 is either zero or very small there, we set $c_s^2 k_r^2 = \omega^2 - S_\ell^2$. The eigenfrequencies are then found by setting $\int k_r dr \approx n_p \pi$. In the extreme limit of $\omega^2 \gg S_\ell^2$, this simplifies to $n_p \pi = \omega \int dr / c_s$, where the integral extends over the outer parts of the star where $\omega^2 > S_\ell^2$. Tradition is to write this as $\nu = n_p \Delta\nu$, where the “large spacing” $\Delta\nu$ is defined with the integral over the whole star,

$$\Delta\nu^{-1} = 2 \int_0^R \frac{dr}{c_s}, \quad (4)$$

a reasonably accurate representation.

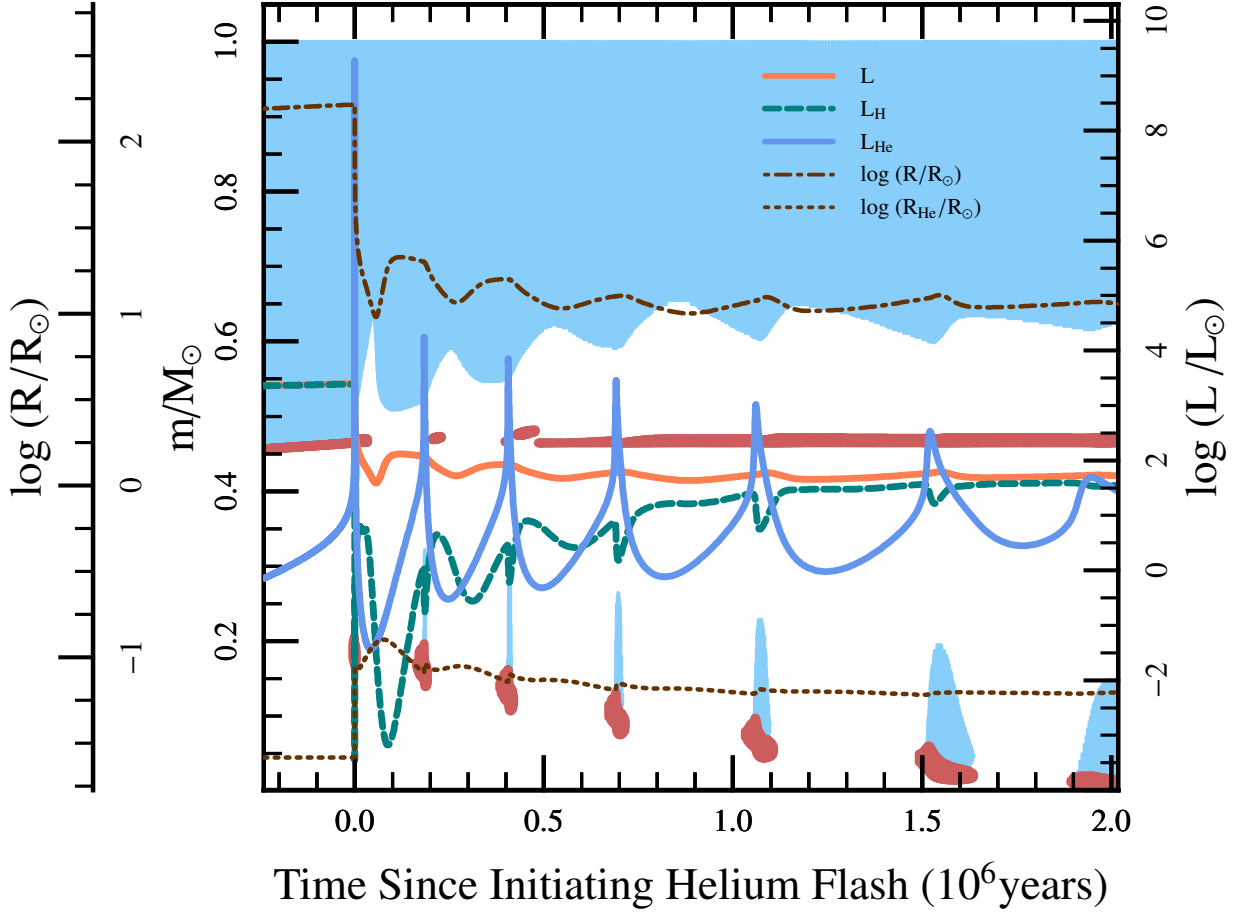


Fig. 2.— Properties of a $M = 1.0M_{\odot}$ star for the 2 Myr core flash phase. The blue shaded regions show where convection is present in mass coordinates, whereas the orange shaded regions are where nuclear burning yields $> 1000 \text{ ergs gr}^{-1} \text{ s}^{-1}$. The stellar luminosity is shown by the orange solid line, whereas the H (He) burning luminosities are shown by the green dashed (blue solid) lines. The stellar radius, R , is shown by the brown dot-dashed line, and the dotted brown line shows the He core radius.

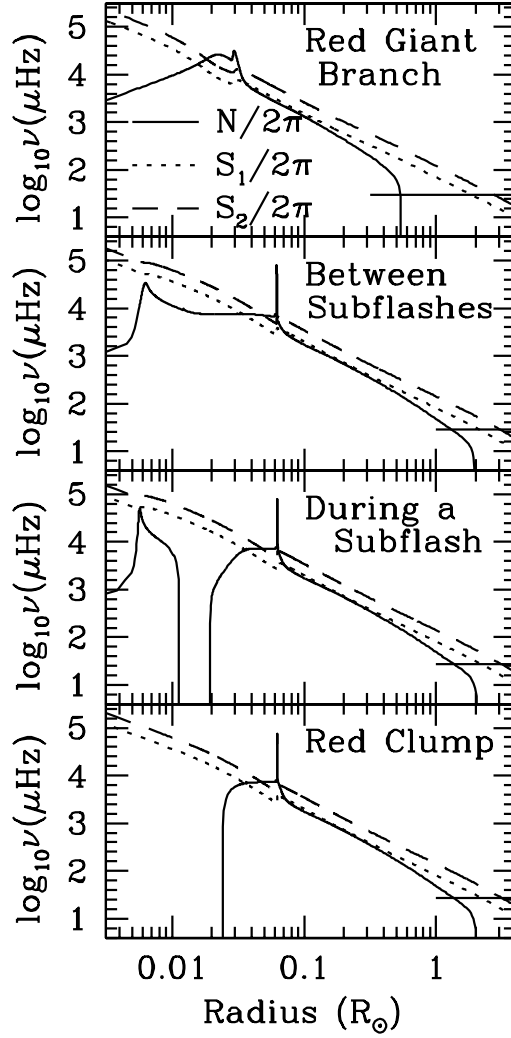


Fig. 3.— Propagation diagrams for a $M = 1.0M_{\odot}$ star at four different stages of evolution (described in text), all when $\Delta\nu = 4\mu\text{Hz}$. The Brunt-Väisälä frequency, $N/2\pi$ (solid lines), and Lamb frequencies $S_1/2\pi$ (dotted lines) and $S_2/2\pi$ (dashed lines) are shown. The thin horizontal line is at $\nu_{\text{max}} \approx 28\mu\text{Hz}$. From top to bottom, these models have $L/L_{\odot} = 41.6, 50.6, 51.1\&50.8$, and $R/R_{\odot} = 10.9, 11.2, 11.2\&11.2$.

Modes supported by the internal buoyancy (i.e. g-modes) propagate in the stellar interior, where $\omega^2 < N^2$ and $\omega^2 < S_\ell^2$. As evident from Figure 3, these inequalities are strong for frequencies $\sim \nu_{\max}$, yielding $k_r^2 \approx \ell(\ell+1)N^2/r^2\omega^2$. The high radial order ($n_g \gg 1$) g-modes then have $n_g\pi = (\ell(\ell+1))^{1/2} \int N d\ln r / \omega$, yielding $\nu^{-1} = n_g \Delta P_g$, with ΔP_g being the period spacing. For $\ell = 1$, this is

$$\Delta P_g(\ell = 1) = \frac{2^{1/2}\pi^2}{\int N d\ln r}. \quad (5)$$

At ν_{\max} , $n_g \approx 1/(\nu_{\max}\Delta P_g) > 100$, safely in the WKB limit. The integral $\int N d\ln r$ extends over the region where $\omega^2 < N^2$ and $\omega^2 < S_\ell^2$.

Now consider how ΔP_g and $\Delta\nu$ evolve during the core flash phase. The KH contraction after the initiating flash triggers a rapid decrease to $R \approx 11R_\odot$, and the increase of $\Delta\nu$ evident in the second panel of Figure 4. Thereafter, the value of $\Delta\nu$ simply responds to the mild radius changes during subsequent subflashes. The He core radius expansion and outer envelope contraction triggered by the initiating He flash leads to an outer envelope structure during the $t_f \approx 2$ Myr that is nearly the same as that on the red clump. Indeed, the profiles of N^2 and S_ℓ^2 in Figure 3 for the bottom three panels (all after the initiating flash) are nearly identical for $r > 0.04R_\odot$.

The prime property that is changing over the 2 Myr is the He core, as it undergoes additional subflashes that lift the degeneracy of the deep interior. The $\ell = 1$ g-mode period spacings for the models in Figure 3 are $\Delta P_g = 61.2$ s for the RGB, $\Delta P_g = 73$ s for the core flash phase model between subflashes (second panel), and $\Delta P_g = 255$ s for the red clump. During the convective He burning shell subflashes (less than 10% of the He core flash phase, so $< 2 \times 10^5$ years), an intervening evanescent zone appears in the core (see third panel in Figure 3). Though coupling through this zone is possible (see below), we calculated the period spacing assuming that only the outer g-mode cavity is relevant, giving $\Delta P_g \approx 250 - 270$ s during each sub-flash. As evident in the third panel of Figure 4, the existence of a degenerate core with $N^2 > 0$ during the most of the core flash period keeps $\Delta P_g < 100$ s. The fully convective He burning core of the red clump is what causes the increase to $\Delta P_g = 255$ s (Christensen-Dalsgaard 2011a) at the end of Figure 4.

The $\ell = 1$ mixed modes are more likely to be detected when the coupling through the outer evanescent region (the region in the star where $\omega^2 > N^2$ and $\omega^2 < S_\ell^2$ so that $k_r^2 < 0$) is strong. In the WKB limit, the ratio of the mode amplitudes (and also location of the mode energy) between the two turning points, the inner one at r_1 (where $\omega^2 < N^2$ first occurs) and the outer one at r_2 (where $\omega^2 > S_\ell^2$ first occurs) is largely determined by $I = \int_{r_1}^{r_2} k_r dr$, but

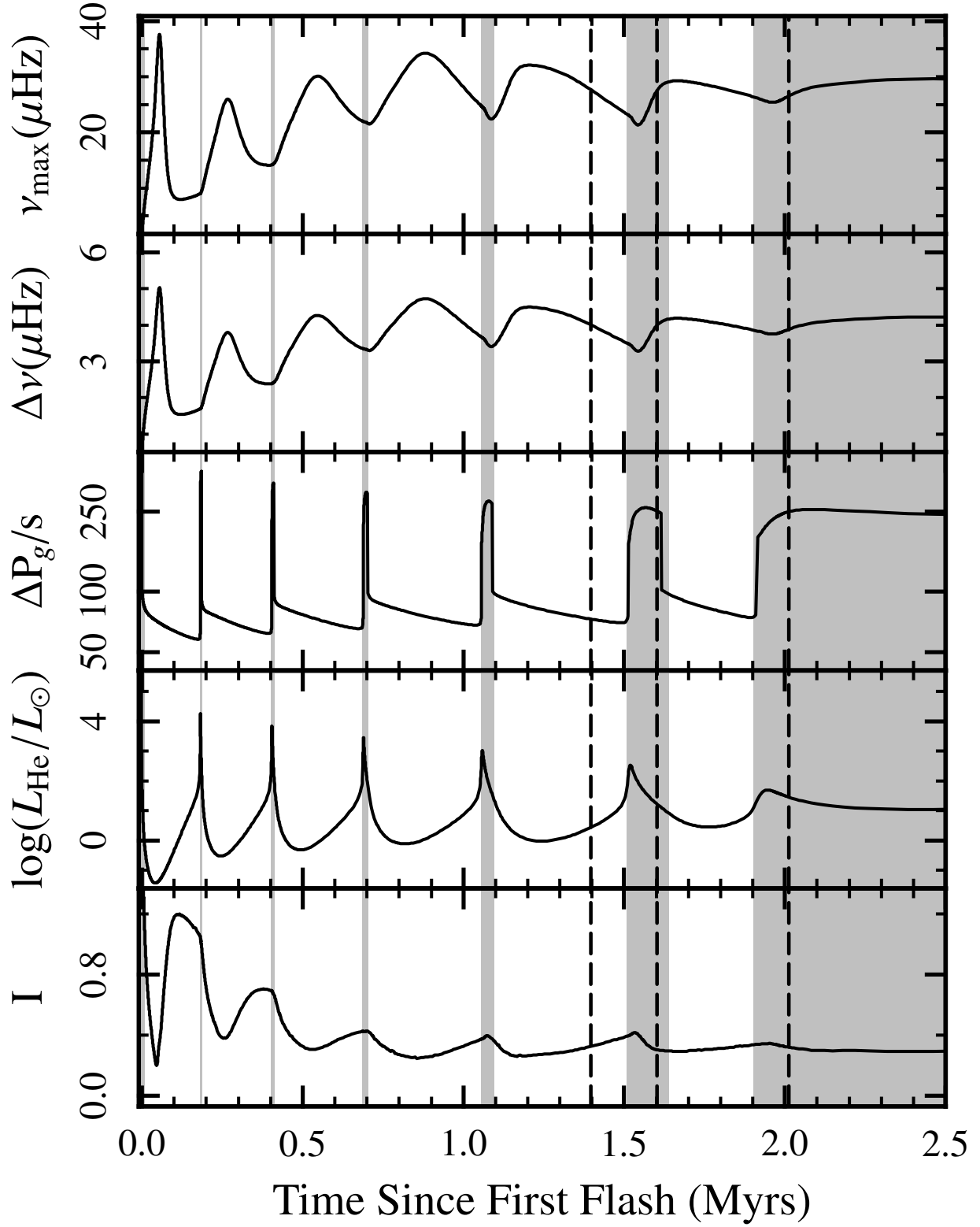


Fig. 4.— Seismic properties during the core flash, with vertical grey regions showing sub-flashes. From top to bottom, the panels show ν_{\max} from equation (1), $\Delta\nu$ from equation (4), ΔP_g from equation (5), the Helium burning luminosity L_{He} , and the evanescent integral I . The vertical dashed lines denote the times for the bottom three panels of Figure 3.

also depends on r_1 and r_2 (Aerts et al. 2010).¹ The coupling of the $\ell = 1$ modes is stronger than that of $\ell = 2$ simply because the outer turning point is closer to the core for $\ell = 1$ (Christensen-Dalsgaard 2004; Dupret et al. 2009). The values of I (calculated at $\nu = \nu_{\max}$) for the models in Figure 3 are $I = 1.26$ for the RGB, and $I \approx 0.3$ for the other three models (which have nearly identical outer envelopes). The bottom panel of Figure 4 shows that I changes little over the 2 Myr, giving us confidence that the seismic probe of the core will be as fruitful for the He core flash stars as the red clump.

We have not fully investigated the mode structure during the subflashes. However, a few things can be said. The first is that an additional inner evanescent zone appears during subflashes (the region at $0.0115 < r/R_\odot < 0.0192$ in the third panel of Figure 3) splitting the g-mode cavity into two zones, each with their own distinct period spacing. This adds an additional evanescent integral $I_i \approx [\ell(\ell + 1)]^{1/2} d \log r \approx 0.72$ that must be accounted for in the observable mode structure. Due to that extra penalty, we chose to display (in Figure 4) the period spacing during the subflashes as that of the outermost g-mode cavity. If the inner cavity proves to be adequately coupled, these extra modes would cause oscillations in the observed period spacing diagram. That full analysis awaits our future efforts.

4. Detecting the Core Flash Phase

Our results are best seen in relation to the observational work performed by Bedding et al. (2011) and Mosser et al. (2011a). Their secure detection of mixed modes and measurement of their period spacing, ΔP_{obs} , led to a clear distinction (see Figure 5) of RGB stars (blue points) from the red clump stars (red points) of $M \lesssim 2M_\odot$ and the extended red clump (yellow points). The evolution of ΔP_g for our $1.0M_\odot$ (green lines) and a $1.8M_\odot$ (black lines) models are shown in Figure 5 as a dashed line for the RGB, a solid line during the core flash and a short-dashed line for the core He burning phase.

Bedding et al. (2011) discussed the challenge of securely inferring ΔP_g when only a few mixed modes are observed (see also Mosser et al. (2011a); Christensen-Dalsgaard (2011b)). In particular, they found that the measured spacing, ΔP_{obs} , would be less than ΔP_g by a factor of 1.3 – 1.6. Such a need for scaling is evident along the RGB, and will be best resolved by longer duration *Kepler* data that reveals additional mixed modes. This should prove possible given their much longer expected lifetimes (Dupret et al. 2009).

Stars undergoing the core flash occupy a distinct region in Figure 5. The only other

¹In the plane-parallel limit (e.g. $r_2 - r_1 \ll r_2$), the mode amplitude ratio is $\propto \exp(\pm I)$.

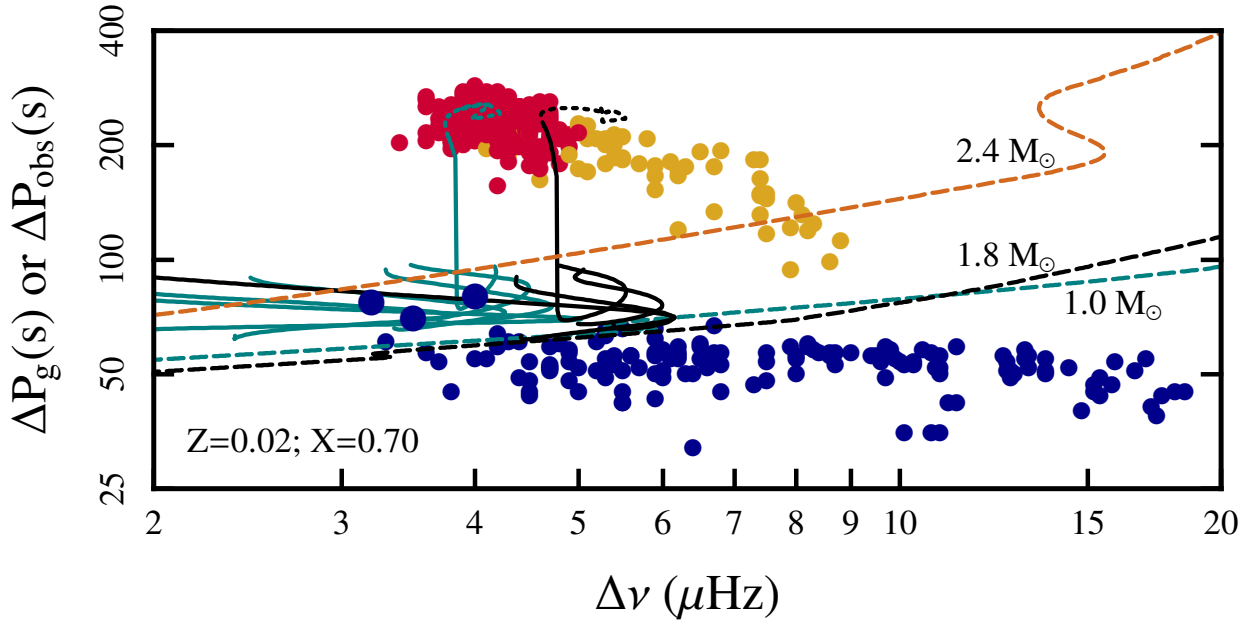


Fig. 5.— Evolution of $1.0M_{\odot}$ (green) and $1.8M_{\odot}$ (black) red giants through the helium core flash in $\Delta\nu - \Delta P_g$ space. The RGB of a $2.4M_{\odot}$ star is shown by an orange line. The dashed lines are the RGB phase, whereas the solid line is the core flash (with the rare excursions during subflashes omitted) and short-dashed the He burning stage. The colored data points are ΔP_{obs} from Bedding et al. (2011).

models that traverse this region are $M > 2.0M_{\odot}$ RGB stars, and potentially AGB stars, both reasonably rare instances that will need to be observationally distinguished. The simplest technique is to use the measured ν_{\max} values, as $\nu_{\max} \approx 38$ Hz for the $2.2M_{\odot}$ and $2.4M_{\odot}$ RGB models, whereas $\nu_{\max} < 32$ Hz during the core flash for the $1.0M_{\odot}$ model of Figure 4. All objects with $70 \text{ s} < \Delta P_g < 200 \text{ s}$ and $2\mu\text{Hz} < \Delta\nu < 6\mu\text{Hz}$ are worthy of a serious analysis to see if they are explained as $\approx 1M_{\odot}$ core flash stars rather than $> 2M_{\odot}$ RGB stars. We highlight three such candidates in Figure 5 by slightly enlarging their blue points. Since ΔP_{obs} is always less than ΔP_g , these points could only move upwards in this diagram, placing them securely in the region of interest. There are 193 red clump stars in this figure, so we expect about $193/35 \approx 5$ flashing stars, consistent with the few “outliers” in this early data set. Miglio et al. (2009) showed that the expected metallicity of most of the CoRoT red giants is near solar, with a few as low as one-tenth solar. Our MESA runs for one-tenth solar occupy a comparable part of this diagram, though they go to slightly higher values of $\Delta\nu$ during the flash due to reaching a lower luminosity during KH contraction.

There is much to be learned from the asteroseismic discovery and analysis of a star undergoing the core flash phase. It would be an immediate confirmation of the ~ 2 Myr duration of the event; eliminating the alternate possibilities of more dynamical outcomes. Study and analysis of the g-modes may reveal the specific stage of evolution for such a star in the 2 Myr phase. Any possible inferences regarding the rotation rate of the core during these 2 Myrs would be especially valuable, as the short timescales may not allow for perfectly rigid core rotation. Another path to detection of this rare phase was highlighted by Silva Aguirre et al. (2008), who noted that RGB stars with substantial mass loss will cross the RR Lyrae instability strip on their way to the horizontal branch. Those stars would then exhibit a detectable pulsation period change due to their secular evolution.

Additional calculations are certainly needed, both to fully explore lower metallicities, as well as to see how additional mixing mechanisms (e.g. thermohaline) may impact the qualitative evolution. Fully consistent pulsation calculations are needed, both to confirm the WKB estimates here, but also to provide damping times and to explore the interesting periods of subflashes (only relevant for $\approx 2 \times 10^5$ years) that may prove detectable if the sample size of red giants with measured ΔP_g gets large enough.

We thank T. Bedding, T. Brown, J. Christensen-Dalsgaard and V. Silva Aguirre for discussions. This work was supported by the NSF through grants PHY 05-51164 and AST 11-09174 and by support for K.M and P.J.M. through the Worster Family Summer Fellowship fund.

REFERENCES

- Aerts, C., Christensen-Dalsgaard, J., & Kurtz, D. W. 2010, *Asteroseismology*, ed. Aerts, C., Christensen-Dalsgaard, J., & Kurtz, D. W.
- Aizenman, M., Smeyers, P., & Weigert, A. 1977, *A&A*, 58, 41
- Baglin, A., Auvergne, M., Barge, P., Deleuil, M., Michel, E., & The CoRoT Exoplanet Science Team. 2009, in *IAU Symposium*, Vol. 253, *IAU Symposium*, 71–81
- Baudin, F. et al. 2011, *A&A*, 529, A84+
- Beck, P. G. et al. 2011, *Science*, 332, 205
- Bedding, T. R. et al. 2010, *ApJ*, 713, L176
- . 2011, *Nature*, 471, 608
- Borucki, W. et al. 2009, in *IAU Symposium*, Vol. 253, *IAU Symposium*, 289–299
- Brown, T. M., Gilliland, R. L., Noyes, R. W., & Ramsey, L. W. 1991, *ApJ*, 368, 599
- Christensen-Dalsgaard, J. 2004, *Sol. Phys.*, 220, 137
- . 2011a, *ArXiv e-prints* 1106.5946
- . 2011b, *ArXiv e-prints* 1110.5012
- De Ridder, J. et al. 2009, *Nature*, 459, 398
- di Mauro, M. P. et al. 2011, *MNRAS*, 415, 3783
- Dominguez, I., Chieffi, A., Limongi, M., & Straniero, O. 1999, *ApJ*, 524, 226
- Dupret, M.-A. et al. 2009, *A&A*, 506, 57
- Dziembowski, W. A., Gough, D. O., Houdek, G., & Sienkiewicz, R. 2001, *MNRAS*, 328, 601
- Ferguson, J. W., Alexander, D. R., Allard, F., Barman, T., Bodnarik, J. G., Hauschildt, P. H., Heffner-Wong, A., & Tamanai, A. 2005, *ApJ*, 623, 585
- Grevesse, N., & Sauval, A. J. 1998, *Space Sci. Rev.*, 85, 161
- Hekker, S. et al. 2011, *MNRAS*, 414, 2594
- . 2009, *A&A*, 506, 465

- Huber, D. et al. 2011, ArXiv e-prints
- . 2010, ApJ, 723, 1607
- Iben, I., & Renzini, A. 1984, Phys. Rep., 105, 329
- Iglesias, C. A., & Rogers, F. J. 1996, ApJ, 464, 943
- Jiang, C. et al. 2011, ArXiv e-prints
- Kjeldsen, H., & Bedding, T. R. 1995, A&A, 293, 87
- Miglio, A. 2011, ArXiv e-prints 1108.4555
- Miglio, A. et al. 2009, A&A, 503, L21
- Mocák, M., Müller, E., Weiss, A., & Kifonidis, K. 2008, A&A, 490, 265
- . 2009, A&A, 501, 659
- Montalbán, J., Miglio, A., Noels, A., Scuflaire, R., & Ventura, P. 2010, ApJ, 721, L182
- Mosser, B. et al. 2011a, A&A, 532, A86+
- . 2011b, A&A, 525, L9+
- . 2010, A&A, 517, A22+
- Osaki, J. 1975, PASJ, 27, 237
- Paxton, B., Bildsten, L., Dotter, A., Herwig, F., Lesaffre, P., & Timmes, F. 2011, ApJS, 192, 3
- Rogers, F. J., & Nayfonov, A. 2002, ApJ, 576, 1064
- Salaris, M., Cassisi, S., & Weiss, A. 2002, PASP, 114, 375
- Scuflaire, R. 1974, A&A, 36, 107
- Serenelli, A., & Weiss, A. 2005, A&A, 442, 1041
- Serenelli, A. M., & Fukugita, M. 2005, ApJ, 632, L33
- Shen, K. J., & Bildsten, L. 2009, ApJ, 699, 1365
- Silva Aguirre, V., Catelan, M., Weiss, A., & Valcarce, A. A. R. 2008, A&A, 489, 1201

- Stello, D., Chaplin, W. J., Basu, S., Elsworth, Y., & Bedding, T. R. 2009, MNRAS, 400, L80
- Thomas, H.-C. 1967, ZAp, 67, 420
- Timmes, F. X., & Swesty, F. D. 2000, ApJS, 126, 501
- Unno, W., Osaki, Y., Ando, H., Saio, H., & Shibahashi, H. 1989, Nonradial oscillations of stars, ed. Unno, W., Osaki, Y., Ando, H., Saio, H., & Shibahashi, H.